Available online at www.sciencedirect.com
ScienceDirect
Journal of the European Ceramic Society 27 (2007) 1193–1197
www.elsevier.com/locate/jeurceramsoc

Relationships between dielectric breakdown resistance and charge transport in alumina materials—Effects of the microstructure

M. Touzin [a], D. Goeuriot [a,*], H.-J. Fitting [b], C. Guerret-Piécourt [c], D. Juvé [c], D. Tréheux [c]

[a] *Centre Sciences des Matériaux et des Structures, Ecole Nationale Supérieure des Mines, UMR 5146-CNRS, 158 cours Fauriel, F-42023 Saint-Etienne Cedex 2, France*
[b] *Physics Department, University of Rostock, Universitätsplatz 3, D-18051 Rostock, Germany*
[c] *Laboratoire de Tribologie et Dynamique des Systèmes, Ecole Centrale de Lyon, 36 Avenue Guy de Collongue, F-69134 Ecully Cedex, France*

Available online 23 June 2006

Abstract

Dielectric breakdown is the main cause of insulator degradation. Breakdown strength strongly depends on materials microstructure (grain size, grain boundaries nature,. . .) [Liebault, J., Vallayer, J., Goeuriot, D., Tréheux D., Thévenot, F., How the trapping of charges can explain the dielectrics breakdown performance of alumina ceramics, *J. Eur. Ceram. Soc.*, 2001, **21**, 389–397; Si Ahmed, A., Kansy, J., Zarbout, K., Moya, G., Liebault, J., Goeuriot, D., Microstructural origin of the dielectric breakdown strength in alumina: a study by positron lifetime spectroscopy, *J. Eur. Ceram. Soc.*, 2005, **25**, 2813–2816]. The experimental study of these materials behaviour towards charge injection was performed by the scanning electron microscopy mirror effect (SEMME) method. It allows to measure the amount of injected charges finally trapped in the insulator. In order to explain the experimental results, we developed an iterative computer simulation of the self-consistent charge transport in bulk alumina samples during electron beam irradiation, based on a new flight-drift model (FDM). Ballistic and drift electron and hole transport as well as their recombination, trapping and detrapping (due to temperature and electric field) are taken into account. As a main result the time dependent secondary electron emission rate and the spatial distributions of currents, charges, field and potential are obtained. The analysis of these two kinds of results allowed us to identify the effect of the microstructure on the behaviour of the injected charges in the insulator and then to propose some mechanisms depending on the temperature leading to a good dielectric breakdown resistance. Indeed, at room temperature a huge localisation of charges limits further injection into the sample that permits to delay breakdown. On the other hand, when the temperature increases, the efficiency of the charge spreading behaviour is improved, leading to a higher dielectric breakdown strength.

Keywords: Grain boundaries; Interfaces; Dielectric properties; Al_2O_3

1. Introduction

The dielectric properties of insulators, and specially dielectric strength, strongly depend on defects. Defects are considered as sites where polarizability is modified and where charge and energy localisation can occur. In ceramics, such defects can be porosity, grain boundaries or interfaces with a secondary phase.

In this work, a correlation is proposed between breakdown strength, trapping of charges and materials microstructure. The amount of defects is controlled by modifying the grain size of materials, i.e. the grain boundaries density or the crystallization state of the secondary phase. The influence of these defects on the electrical conductivity and the breakdown strength of alumina materials has been shown by several authors.[3–6]

Studied materials are alumina ceramics with around 6–8% of sintering additives (minerals containing Al_2O_3, MgO, SiO_2 and CaO). The intergranular phase is controlled by raw alumina grain size and sintering conditions: all the materials contain a small amount of spinel phase ($MgAl_2O_4$) after sintering, and the remaining intergranular phase is vitreous or crystallized. Microstructural parameters and breakdown strength at room temperature are shown in Table 1.

Considering that interfaces play the main role in trapping phenomena, it is useful to classify the materials versus this parameter, from the microstructures described before:

- Comparison of materials 1–3: they present almost the same grain boundary composition, so the same types

* Corresponding author. Tel.: +33 4 77 42 01 92; fax: +33 4 77 42 02 49.
E-mail address: dgoeurio@emse.fr (D. Goeuriot).

0955-2219/$ – see front matter © 2006 Elsevier Ltd. All rights reserved.
doi:10.1016/j.jeurceramsoc.2006.05.047

Table 1
Microstructural chararacteristics and dielectric breakdown strength at room temperature (about 300 K)

Reference	Secondary phase	Average grain size (μm)	Breakdown strength, E_b (kV/mm)
1	Glass + $\varepsilon MgAl_2O_4$	1.8	15.1 ± 0.8
2	Glass + $\varepsilon MgAl_2O_4$	2.1	14.3 ± 0.6
3	Glass + $\varepsilon MgAl_2O_4$	3.4	14.3 ± 0.4
4	Anorthite + εglass + $\varepsilon MgAl_2O_4$	2.2	14.9 ± 0.9

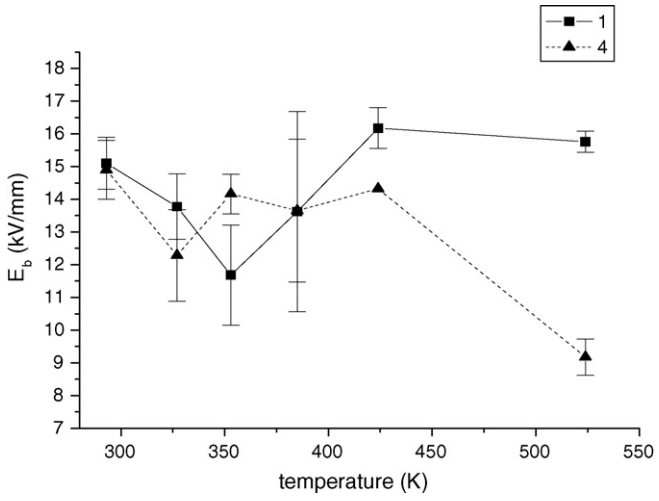

Fig. 1. Breakdown strength evolution with temperature for materials 1 and 4.

of interfaces (Al_2O_3/Al_2O_3, Al_2O_3/glass, $Al_2O_3/MgAl_2O_4$, glass/$MgAl_2O_4$); but the lower the grain size, the higher the interfaces number, so material 1 presents the higher trap content.

- Comparison of materials 1 and 4: material 4 presents a grain size slightly higher than that of material 1, but grain boundaries contain small anorthite particles that leads to new kinds of interfaces (Al_2O_3/anothite, anorthite/anorthite, anorthite/glass).

In conclusion, it can be supposed that materials 1 and 4 present more traps than materials 2 and 3.

Fig. 1 shows the evolution of the dielectric breakdown strength with temperature for materials 1 and 4. Materials 1 and 4 present the highest breakdown resistance at room temperature. The evolution of the breakdown strength with temperature is different for these two materials: at high temperature, we only observe a decrease of dielectric strength for material 4, not for material 1. That shows the huge influence of microstructure on breakdown resistance and its evolution with temperature.

2. Numerical simulation of the charge transport

The flight-drift model (Fig. 2) developed by Fitting allows us to simulate the charge transport and charging-up of insulating Al_2O_3 samples during electron bombardment. This model is an evolution of the one used by Meyza et al.[7,8] to calculate the secondary electron emission and self-consistent charge transport and storage in alumina bulk insulators. In this new model, we consider, in addition to the electrons and holes ballistic current, a drift current due to the internal electrical field. Moreover, we take into account the role of the temperature on the charges detrapping by considering the Poole–Frenkel (PF) effect.

Fig. 3 shows the evolution during irradiation of the surface potential and the secondary electron emission at room temperature. The surface potential strongly decreases during the first 20 ms of irradiation and then remains constant at a very negative value (∼−24 keV). This negative surface potential leads to a injection limitation of new electrons. The secondary electron emission rate starts from 0.45 to a little bit higher than 1 and then stabilizes at 1, meaning that an equilibrium between injection and emission is reached. The charge repartition at room temperature has also been calculated, it is presented in Fig. 4.

We can notice at the extreme surface of the sample an excess of positive charges controlled by the secondary electron emission. Deeper in the material, the total charge is negative and separated into two populations because of the internal electrical field sign change. At 300 K, charges tend to be stabilized in the material, the repartition doesn't move so much any more after 80 ms of injection.

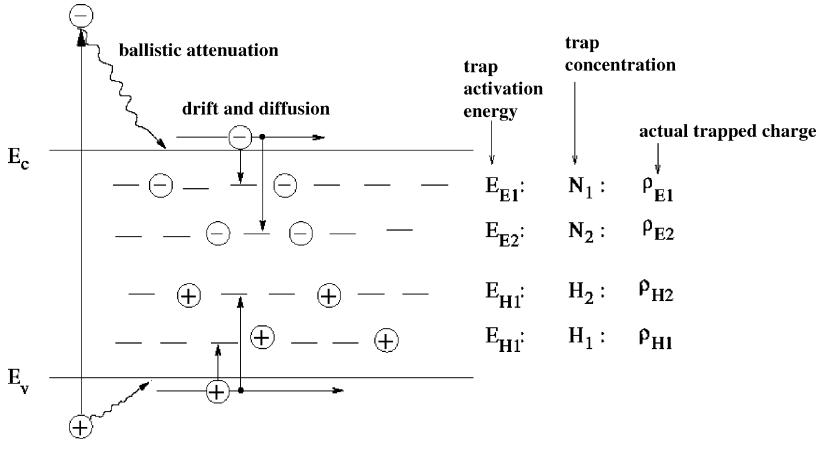

Fig. 2. Energy band scheme with excited, drifting and trapped electrons and holes.

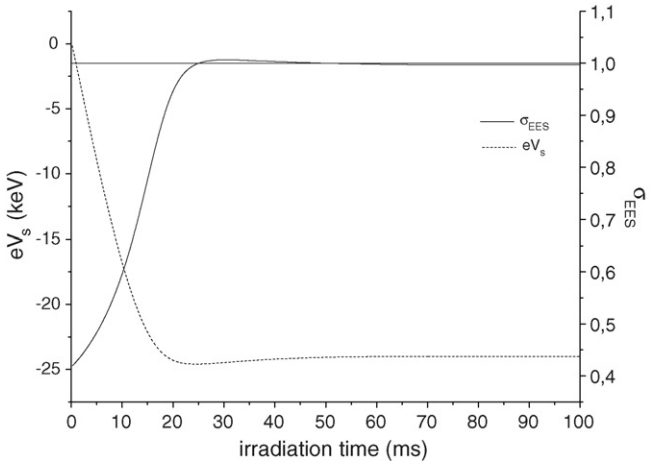

Fig. 3. Evolution with time of the surface potential and secondary electron emission, $T = 300$ K, $E_0 = 30$ keV, $j_0 = 10^{-5}$ A/cm^2.

The evolution with temperature of this distribution is shown in Fig. 1. By comparing Figs. 4b and 5 we see that at 600 K, charges are not stabilized, they keep on spreading into the sample after 100 ms of irradiation. If we compare the charge repartition at 100 ms (Fig. 5b) for three different temperatures,

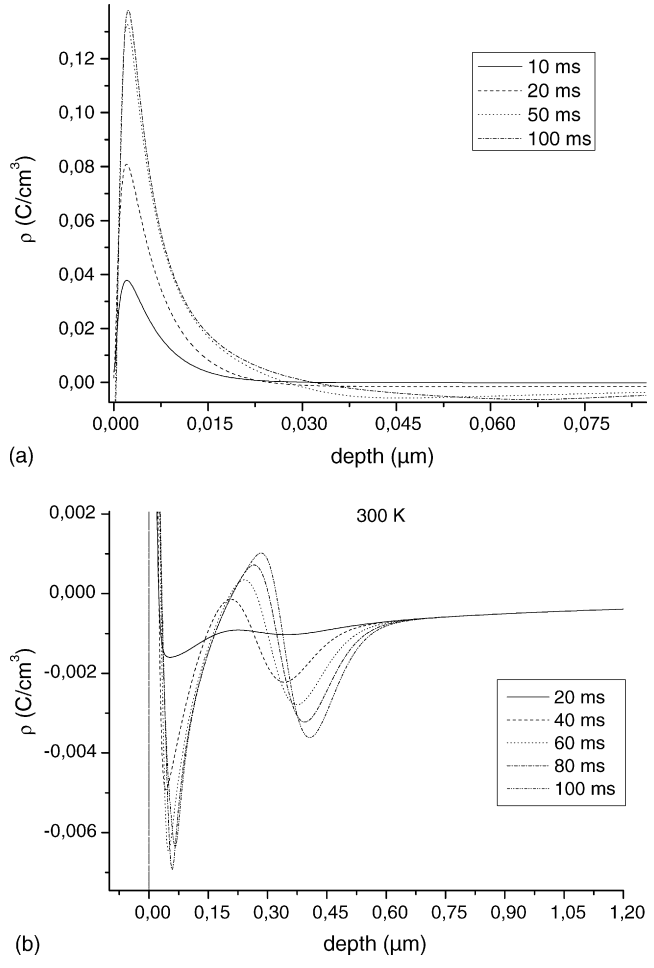

Fig. 4. Evolution of the charge distribution with time at room temperature: (a) up to 75 nm and (b) up to 1.2 μm.

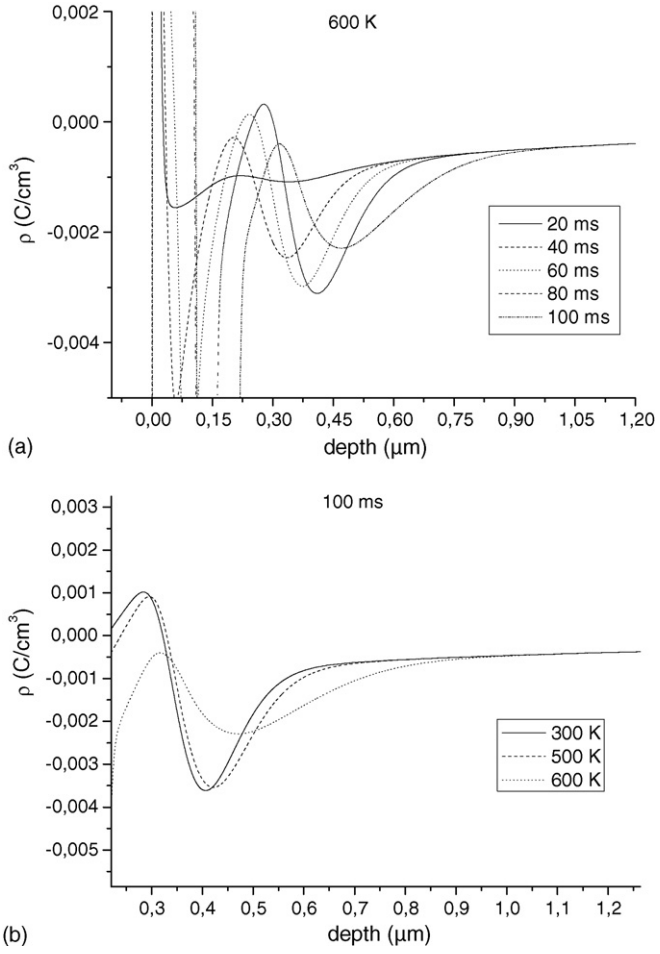

Fig. 5. Evolution of the charge distribution: (a) with time at 600 K and (b) with the temperature after 100 ms of irradiation).

we see that the higher the temperature, the deeper charges spread.

The temperature increase leads to a transition from a charge stabilization behaviour to a charge spreading one.

3. Experimental results

The possibility to create and store charges in ceramics can be measured experimentally using a scanning electron microscope equipped with a cold-hot stage.[9] During injection using the SEM electron beam at high energy (30 kV), negative trapped charges appear in the insulating material that produce positive "influence" charges in all conductor pieces of the SEM chamber. The current measured between the holder and the ground is directly proportional to the quantity of charges Q inside the material. After injection, the observation of the sample surface at low accelerating voltage (few 100 V) can reveal "a mirror effect" if the trapped charge Q_S is sufficiently concentrated to create an electric field strong enough to deflect the incoming electrons, as a convex mirror with light. This effect permits to evaluate the quantity of stabilised charge Q_S and then by calculating the ratio $((Q_s/Q) \times 100 = R)$, the stabilised charge R rate is obtained.

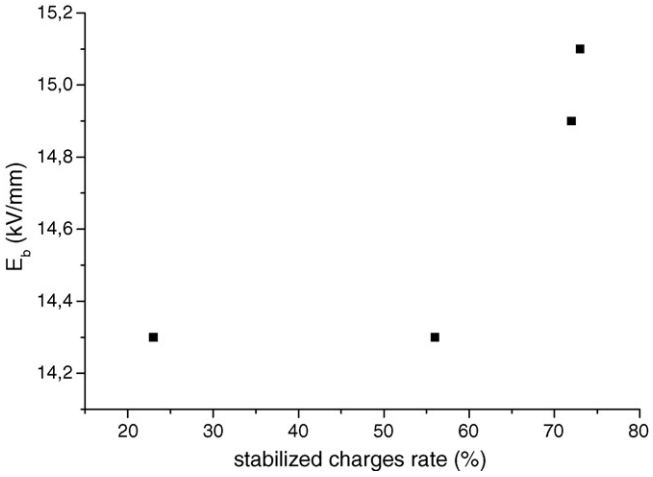

Fig. 6. Breakdown field strength E_b evolution as a function of the stabilised charge rate R at 25 °C (about 300 K).

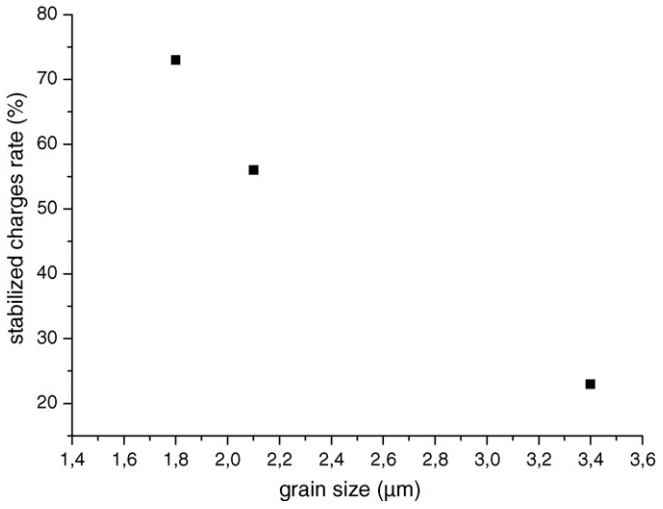

Fig. 7. Stabilized charge rate evolution with alumina grain size for "vitreous materials" 1–3.

3.1. At room temperature

The breakdown strength evolution in dependence on the stabilisation rate is plotted on Fig. 6.

Despite dielectric breakdown strength values present high dispersion, the mean values obtained for the four material permit to highlight tendencies: Fig. 6 shows that the two materials presenting the highest stabilisation rates ($R \sim 70\%$) are those that offer the best resistance to dielectric breakdown at room temperature: $E_b = 14.9$ and 15.1 kV/mm, respectively. An important amount of stabilised trapped charges leads to the creation of a very negative surface potential that limits further charge injection and then delays the dielectric breakdown. It seems that a stabilized charge rate R below 60% is not high enough to create a surface potential negative enough to block further electron injection. In this case R has no more influence on E_b.

Grain size is inversely proportional to grain boundaries density that are considered as charge trapping sites. Stabilised charge rates versus grain size of aluminas with an intergranular phase mainly vitreous (called below "vitreous materials") are plotted in Fig. 7.

The decrease of R with grain size confirms that grain boundaries are the main trapping sites in the "vitreous materials".

At room temperature, materials 1 and 4 are those that have the best resistance to dielectric breakdown. These materials present a great defect amount: material 1 has a high grain boundary density, material 4 presents a very high-crystallized secondary phase. These two kinds of microstructure permit to stabilise an important quantity of charges within the material at 25 °C (about 300 K). That's why the surface potential adopts a very high negative value that limits charges injection and increases breakdown strength.

3.2. Influence of temperature on charge trapping

By increasing temperature, materials go from a charges stabilisation behaviour to a charge spreading one. Temperature increase leads to a decrease of the effective traps energy. The higher the temperature, the lower the detrapping energy. The evolution of the material behaviour towards charge injection as a function of temperature gives information on trap depths.

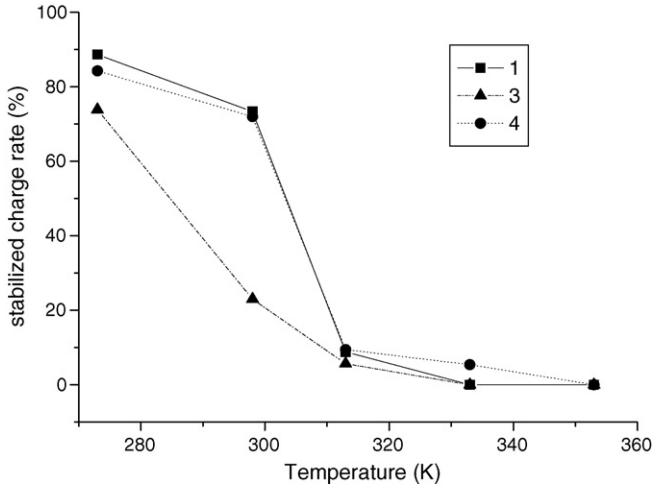

Fig. 8. Stabilized charge rate evolution with temperature for materials 1, 3 and 4.

The stabilized charge rate evolution with temperature is plotted in Fig. 8 for materials 1, 3 and 4.

For the three materials, the main traps are no more active at 40 °C (about 315 K). For the material 3, R is lower for all the tested temperatures: due to the large grain size, the trap concentration is the lowest for this sample. For the high-crystallized secondary phase material 4, a small amount of traps is still active at 60 °C (about 335 K). That means that traps due to intergranular crystallised phases are deeper than those due to intergranular glassy phases.

4. Conclusion

At room temperature, the dielectric breakdown strength is improved in cases when materials are able to stabilise a great amount of charges. This behaviour is observed in materials with

microstructures containing high interface densities. This kind of microstructure corresponds to very fine grains and/or high-crystallized secondary phase materials. Measurements at higher temperature show that traps contained in crystallized secondary phase materials are deeper than those contained in vitreous secondary phase materials. At higher temperature, traps loose their activity and materials adopt a charges spreading behaviour. In this case, the good breakdown resistance would depend on the ability of the charges to diffuse within the materials.

References

1. Liebault, J., Vallayer, J., Goeuriot, D., Tréheux, D. and Thévenot, F., How the trapping of charges can explain the dielectrics breakdown performance of alumina ceramics. *J. Eur. Ceram. Soc.*, 2001, **21**, 389–397.
2. Si Ahmed, A., Kansy, J., Zarbout, K., Moya, G., Liebault, J. and Goeuriot, D., Microstructural origin of the dielectric breakdown strength in alumina: a study by positron lifetime spectroscopy. *J. Eur. Ceram. Soc.*, 2005, **25**, 2813–2816.
3. Pells, G. P., Electrical conductivity of alumina in a irradiation field at temperature up to 700 °C. *Radiat. Eff.*, 1986, **97**, 199–207.
4. Owate, I. and Freer, O. R., The dielectric breakdown of alpha alumina ceramic at room temperature. *Sci. Ceram.*, 1988, **14**, 1013–1018.
5. Carabajar, S., Olagnon, C., Fantozzi, G. and Le Gressus, C., Relations between breakdown field and mechanical properties of ceramics. Conference on Electrical Insulation and Dielectric Phenomena Proceedings. *IEEE Annual Report*, 1995, **11**, 278–281.
6. Morse, C. T. and Hill, G. J., The electric strength of alumina: the effect of porosity. *Proc. Br. Ceram. Soc.*, 1970, **18**, 23–35.
7. Meyza, X., Goeuriot, D., Guerret-Piécourt, C., Tréheux, D. and Fitting, H.-J., Secondary electron emission and self-consistent charge transport and storage in bulk insulators: application to alumina. *J. Appl. Phys.*, 2003, **94**, 5384–5392.
8. Fitting, H.-J., Meyza, X., Guerret-Piécourt, C., Dutriez, C., Touzin, M., Goeuriot, D. and Tréheux, D., Selfconsistent electrical charging in insulators. *J. Eur. Ceram. Soc.*, 2005, **25**, 2799–2803.
9. Vallayer, B., Blaise, G. and Tréheux, D., *Rev. Sci. Instrum.*, 1999, **70**, 3102–3112.